JOURNAL OF MATERIALS SCIENCE **34** (1999) 3447–3453

Application of Raman in phase equilibrium studies: the structures of substitutional solid solutions of KNO_3 by $RbNO_3$

KANGCHENG XU
Chemistry Department, Lanzhou University, Lanzhou, Gansu 730000, People's Republic of China
E-mail: kxu@Lzu.edu.cn

Raman spectroscopy was employed to investigate the KNO_3-$RbNO_3$ system. Raman studies indicated that Rb^+ may substitute K^+ up to 67 mol % in the solid solutions of the KNO_3 II structure (denoted as $K_{1-x}Rb_xNO_3$ (KII)) and up to 80 mol % in the solid solutions of the KNO_3 III structure (denoted as $K_{1-x}Rb_xNO_3$ (KIII)). The substitutional crystals retained the transitions of I to III to II of KNO_3 on cooling and the metastable property of KNO_3 III at room temperature. It was found that rubidium nitrate had a considerable tendency to have the structure of potassium nitrate. This accounts for the fact that larger rubidium ions can replace many more smaller potassium ions in the nitrate than vice versa. When the concentration of rubidium ions was more than 67 mol %, the substituted crystals underwent the mixed structural phase transition of the KNO_3 III structure to the $RbNO_3$ IV structure, and $K_{1-x}Rb_xNO_3$ (KIII) seemed to consist of disordered R3m microstructure.

1. Introduction

Both potassium nitrate and rubidium nitrate can exist in several phases at atmospheric pressure and above room temperature [1, 2]. Due to their special position in the series of alkali metal nitrates, KNO_3 and $RbNO_3$ have more alternative structures at atmospheric pressure [3]. Their structures represent the transition from the structure stable for small cations (R3c) to the structure stable for large cations ($P3_1$). It seemed worthwhile to determine how the polymorphism of potassium nitrate and rubidium nitrate manifests itself in the mixed crystals. The dependence of the structure of the solid solution on the composition will shed light on the trend in the structural changes of alkali metal nitrates.

Two substitutional solid solutions have been reported [4, 5] for solids grown from aqueous solutions of KNO_3-$RbNO_3$ mixtures with variable concentrations: $K_{1-x}Rb_xNO_3$ (KII) for x up to 0.50 and the $K_{1-x}Rb_xNO_3$ crystal with the $RbNO_3$ IV structure ($K_{1-x}Rb_xNO_3$ (RbIV)) for x no less than 0.98. The two phase region was found to extend from 50 to 98 mol % $RbNO_3$. Similar solid-solid solubility was observed [6] for crystals grown from fused mixtures of KNO_3-$RbNO_3$. Electrical conductivity and X-ray measurements indicated [7] that as much as 4 mol % KNO_3 could dissolve in $RbNO_3$ IV at room temperature. The presence of the KNO_3 III structure in the KNO_3 solid solutions was identified from the X-ray diffraction pattern, ferroelectric behaviour and marked volume changes [8].

Phase transition studies by thermal analysis [6, 9] gave different results for the cooling and heating runs. When cooled from the melts, the transition of potassium nitrate from phase I to III was observed for mixtures up to 42 mol % $RbNO_3$ [9]. The two step transition I $\rightarrow$ III $\rightarrow$ II of potassium nitrate was observed only for mixtures containing up to 10 mol % $RbNO_3$. It was assumed that it was difficult for KNO_3 II to dissolve $RbNO_3$. However, the heating studies [6] indicated that the solubility of $RbNO_3$ in KNO_3 II was about 50 mol %.

The binary system of potassium and rubidium nitrate is unusual and interesting because it is one of the few examples in which nonisostructural components form a continuous series of solid solutions. Solid solutions of KNO_3-$RbNO_3$ are also one of the few examples in which larger guest ions can replace many more smaller host ions than vice versa. The difference in solubilities is striking: larger rubidium ions can replace more than half of the smaller potassium ions in potassium nitrate while smaller potassium ions can only replace about 5 mol % rubidium ions. Finally, it was noted [6] that the two high temperature transitions of rubidium nitrate disappeared between 60 and 90 mol % $RbNO_3$ in the thermal analysis heating run. An independent study was suggested.

In the present work Raman spectroscopy was used to explain the phase diagram of KNO_3-$RbNO_3$ through a study of the structures of the solid solutions from fused mixtures of rubidium and potassium nitrate.

2. Experimental

All the chemicals were analytical grade reagents and were used without further purification.

The nitrates were dried in the oven at 393 K over night. The dried chemicals were weighed at definite ratios, mixed well, and transferred to 5 mm id glass tubes. The mixtures were dried under vacuum for 3 days at 378 K. Then the samples were melted and kept in molten state for 8 h. The quenched samples were obtained when the molten mixtures were taken out of the oven and cooled quickly to the room temperature in the air.

After the Raman measurements the solid samples were reheated to 403 K overnight and then cooled to room temperature very slowly (24 h). These were the annealed samples.

Raman spectra were measured on a Spex 1403 double spectrometer with standard 90° scattering geometry. The 488.0 nm line of a Spectra-Physics argon ion laser (series 2000) was used as the source of excitation. The power level was 200 mW. The slits were set at 200 μm. The data were collected at 0.5 cm^{-1} interval and the integral time for each point was 3 s. For detailed studies in the ν_1 region, the slits were set at 50 μm and the data were collected at 0.2 cm^{-1} interval. MoO_3 was used to calibrate the frequencies. The wavenumbers were accurate to 0.5 cm^{-1}.

3. Raman spectra of the solid solutions of KNO_3-$RbNO_3$

Raman data from the spectra of the quenched samples are collected in Table I and Raman data from the spectra of the annealed samples are collected in Table II. The Raman spectrum of pure $RbNO_3$ was measured for comparison. The Raman data for KNO_3 II and KNO_3 III are taken from reference 10. There are distinct differences in the Raman spectra of the same sample with different thermal histories.

3.1. The quenched samples

The quenched samples with a content of rubidium nitrate up to 80 mol % have the typical Raman features of KNO_3 III (Fig. 1a), indicating the formation of $K_{1-x}Rb_xNO_3$ (KIII). The ν_1 vibration appears at ca. 1054 cm^{-1}, and ν_4 at 717 cm^{-1}. The Raman profile in the ν_3 region presents the typical transverse (TO) and longitudinal (LO) optic Raman features of KNO_3 III [10]: a relative high and sharp peak at 1350 cm^{-1} (TO) and a lower and broad peak at 1440 cm^{-1} (LO). The band at ca. 1430 cm^{-1} is due to the $2\nu_4$ vibration. A single distinct band appears at 1664 cm^{-1} in the $2\nu_2$ region.

There is a small but unambiguous frequency shift in the internal vibrational region of the nitrate ion

TABLE I Observed Raman bands (in cm^{-1}) for the mixed crystals of $K_{1-x}Rb_xNO_3$ (KIII) and $K_{0.05}Rb_{0.95}NO_3$ (RbIV) at 298 K

$K_{1-x}Rb_xNO_3$[a]	External	ν_4	ν_1	ν_3	$2\nu_2$
$x = 1.00$	95, 108	706, 720	1055	1350, 1407, 1440	1673
$x = 0.95$	61, 110	707, 721	1057	1349, 1410, 1440	1674
$x = 0.90$	61, 110	707, 721	1056	1347, 1412, 1435	1674
		714	1049		1661
$x = 0.80$	116	717	1052	1348, 1424, 1435	1662
$x = 0.67$	118	717	1052	1349, 1428, 1437	1663
$x = 0.50$	120	717	1053	1350, 1430, 1438	1664
$x = 0.33$	121	717	1053	1349, 1430, 1439	1663
$x = 0.80$	124	718	1054	1351, 1430, 1441	1665
$x = 0.10$	124	718	1054	1350, 1430, 1440	1664
$x = 0.05$	125	719	1055	1351, 1430, 1442	1664
KNO_3 III[b]	125	717	1053	1348, 1431, 1440	1664

[a]Samples were quenched from the melts and measured at 298 K.
[b]Data from Ref. [10].

TABLE II Observed Raman bands (in cm^{-1}) for the mixed crystals of $K_{1-x}Rb_xNO_3$ (KII) and $K_{0.05}Rb_{0.95}NO_3$ (RbIV) at 298 K

$K_{1-x}Rb_xNO_3$[a]	External	ν_4	ν_1	ν_3	$2\nu_2$
$x = 1.00$	59, 108	706, 720	1055	1350, 1407, 1440	1673
$x = 0.95$	62, 112	708, 722	1057	1350, 1410, 1438	1675
$x = 0.90$	62, 111	707, 721	1057	1348, 1410, 1437	1674
$x = 0.80$	62, 114	707, 721	1057	1348, 1437	1674
		715	1051		1662
$x = 0.67$	41, 79, 120	714	1050	1345, 1357	1650, 1677[c]
$x = 0.50$	43, 80, 121	715	1051	1346, 1358	1650, 1680[c]
$x = 0.33$	45, 81, 121	715	1051	1345, 1359	1650, 1672[c]
$x = 0.20$	47, 82, 122	715	1051	1345, 1359	1654, 1682[c]
$x = 0.10$	49, 82, 123	714	1050	1344, 1358	1650, 1685[c]
$x = 0.05$	50, 83, 123	714	1050	1344, 1358	1651, 1675[c]
KNO_3 II[b]	52, 84, 123	715	1050.5	1344, 1359	1652, 1679[c]

[a]Samples were annealed and measured at 298 K.
[b]Data from Ref. [10].
[c]Broad and weak features from about 1650 to 1680 cm^{-1}.

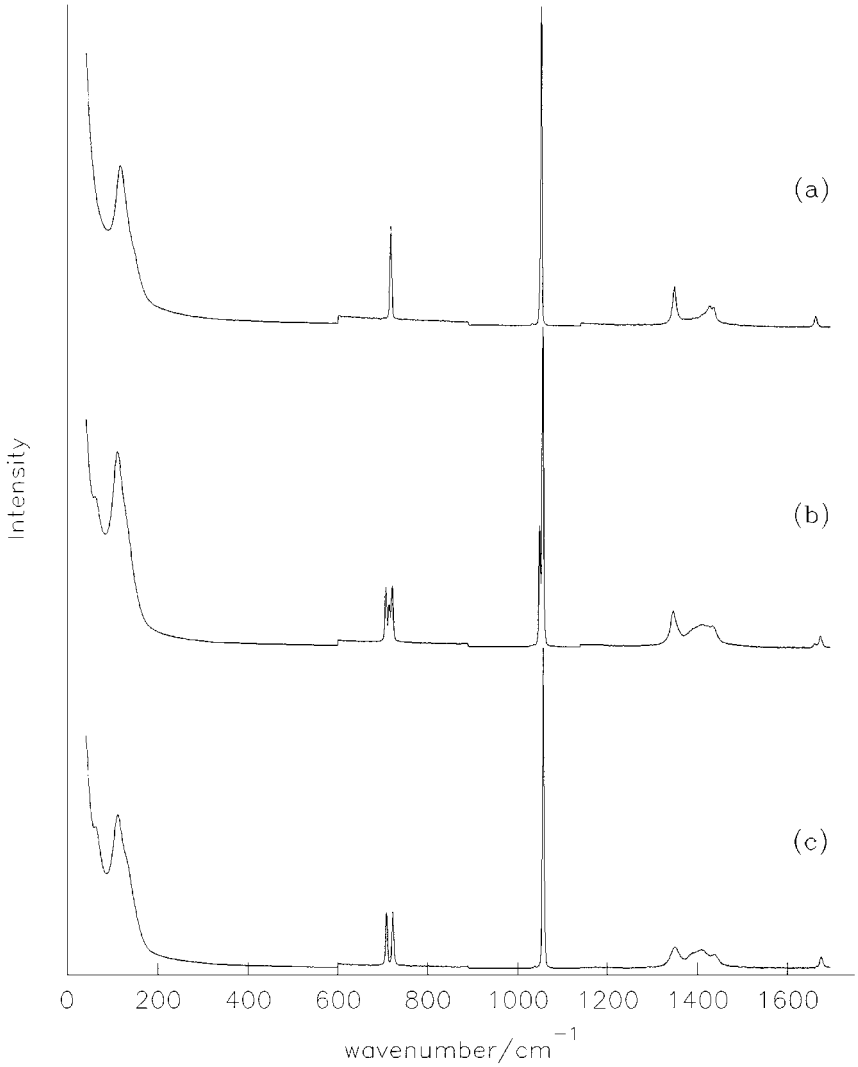

Figure 1 Raman spectra of the quenched $K_{1-x}Rb_xNO_3$ measured at 298 K. The intensity in the ν_2, ν_3, ν_4 and $2\nu_2$ regions has been multiplied by 4. (a) $K_{0.20}Rb_{0.80}NO_3$; (b) $K_{0.10}Rb_{0.90}NO_3$; (c) $K_{0.05}Rb_{0.95}NO_3$.

as the amount of $RbNO_3$ in the solid solutions increases (Table I). The ν_1 appears to shift to lower wavenumbers: from 1055 cm^{-1} for $K_{0.95}Rb_{0.05}NO_3$ (KIII) to 1052 cm^{-1} for $K_{0.20}Rb_{0.80}NO_3$ (KIII). The ν_3 vibration also shifts to lower frequencies and the TO-LO splitting seems to decrease a little: 1351 and 1442 cm^{-1} for $K_{0.95}Rb_{0.05}NO_3$ (KIII) and 1348 and 1435 cm^{-1} for $K_{0.20}Rb_{0.80}NO_3$ (KIII). The external mode at 125 cm^{-1} shifted more rapidly on substituting Rb^+ for K^+: 125 cm^{-1} for $K_{0.95}Rb_{0.05}NO_3$ (KIII) and 116 cm^{-1} for $K_{0.20}Rb_{0.80}NO_3$ (KIII) (Table I).

The sample with 95 mol % $RbNO_3$ has the characteristic Raman bands of $RbNO_3$ IV alone (Fig. 1c), suggesting the formation of $K_{0.05}Rb_{0.95}NO_3$ (RbIV). Two peaks at 61 and 110 cm^{-1} appear in the external vibrational region. The ν_1 vibration appears at 1057 cm^{-1} which is 5 cm^{-1} higher than would be expected if the sample were a solid solution with the KNO_3 III structure. There are two distinct bands with very nearly the same intensity in the ν_4 region: 707 and 721 cm^{-1}. Three bands may be distinguished in the ν_3 region: 1349, 1410 and 1440 cm^{-1}. The band at 1674 cm^{-1} is assigned to $2\nu_2$.

The Raman spectrum of $K_{0.10}Rb_{0.90}NO_3$ is a mixture of those of $K_{1-x}Rb_xNO_3$ (KIII) and $K_{0.05}Rb_{0.95}NO_3$ (RbIV) (Fig. 1b): Two bands appear in each of the ν_1 and $2\nu_2$ regions: the stronger bands at 714, 1056, 1674 cm^{-1} due to $K_{0.05}Rb_{0.95}NO_3$ (RbIV), and 707, 721, 1049, 1661 cm^{-1} due to $K_{1-x}Rb_xNO_3$ (KIII). In the ν_3 and external vibrational regions the features due to $K_{1-x}Rb_xNO_3$ (KIII) are too weak to be distinguished from the much stronger features due to $K_{0.05}Rb_{0.95}NO_3$ (RbIV) in the vicinity. To judge from the relative intensities there seems to be more $K_{0.05}Rb_{0.95}NO_3$ (RbIV) which may suggest that the solubility of KNO_3 in $RbNO_3$ is slightly more than 5 mol %.

3.2. The annealed samples

Similarly, the annealed samples can also be classified to three types of solid by the Raman spectra: $K_{1-x}Rb_xNO_3$ (KII) (Fig. 2a), $K_{0.05}Rb_{0.95}NO_3$ (RbIV) (Fig. 2d) and a mixture of the two (Fig. 2b and c). The major difference is that the range for $K_{1-x}Rb_xNO_3$ (KII) reduced a little to $x = 0.67$ from $x = 0.80$ for $K_{1-x}Rb_xNO_3$ (KIII) (Table II) and the Raman features of KNO_3 III are replaced by those of KNO_3 II [10]: two strong bands at ca. 45 and 80 cm^{-1} in the external vibrational region, 1050 and 715 cm^{-1} for ν_1 and ν_4, 1345 and 1358 cm^{-1} with similar intensity in

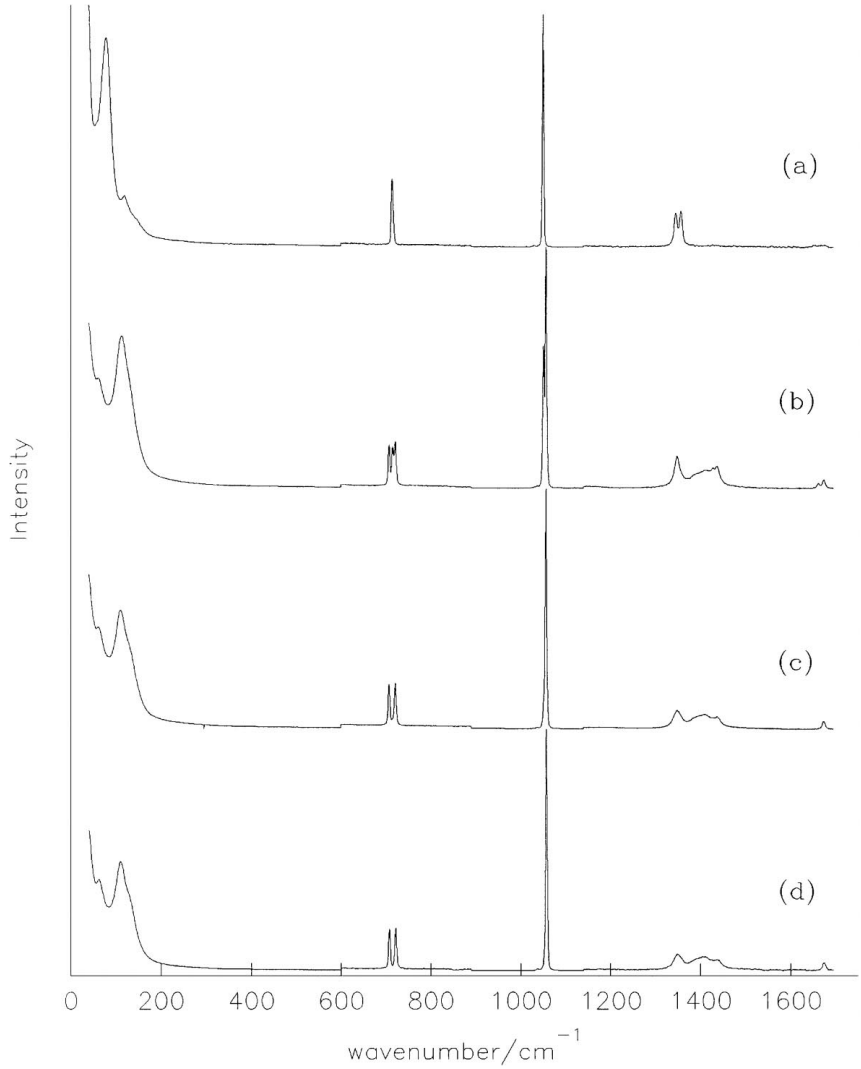

Figure 2 Raman spectra of the annealed $K_{1-x}Rb_xNO_3$ measured at 298 K. The intensity in the ν_2, ν_3, ν_4 and $2\nu_2$ regions has been multiplied by 4. (a) $K_{0.33}Rb_{0.67}NO_3$; (b) $K_{0.20}Rb_{0.80}NO_3$; (c) $K_{0.10}Rb_{0.90}NO_3$; (d) $K_{0.05}Rb_{0.95}NO_3$.

the ν_3 region, weak and obscure features between 1650 and 1680 cm^{-1}.

The presence of rubidium ions in the lattice seems to have little effect on the internal vibrations of nitrate ions in $K_{1-x}Rb_xNO_3$ (KII). The frequency of bands in the ν_1, ν_3, ν_4, and $2\nu_2$ are quite constant from $K_{0.95}Rb_{0.05}NO_3$ to $K_{0.33}Rb_{0.67}NO_3$. On the other hand, the bands of the external modes shift considerably to lower frequencies: from 52 and 83 cm^{-1} for $K_{0.95}Rb_{0.05}NO_3$ to 41 and 79 cm^{-1} for $K_{0.33}Rb_{0.67}NO_3$.

Raman features of the $RbNO_3$ IV structure began to appear for $x = 0.80$. Interestingly, the Raman spectrum of the annealed $K_{0.20}Rb_{0.80}NO_3$ (Fig. 2b) appeared very similar to the spectrum of the quenched $K_{0.10}Rb_{0.90}NO_3$ (Fig. 1b).

4. Discussion

Raman spectroscopy can be employed to determine solubility of a solid solution. The solid solution has only the characteristic Raman bands of the host crystal and the bands due to the solute structure do not appear. The solubility is determined by the first appearance of the Raman bands of the guest crystal structure. Our Raman studies of the KNO_3-$RbNO_3$ system indicated that two kinds of room temperature solid solutions crystallized from the mixed melts. One had the structure of potassium nitrate and the other had the structure of rubidium nitrate. The solubilities were determined by the detailed Raman studies in the most sensitive ν_1 region where a single band indicates a single solid solution and two bands indicate a mixture of solid solutions. It is obvious from the Raman spectra of the quenched samples (Fig. 3I) that the solubility of $RbNO_3$ in KNO_3 III is about 80 mol % and the solubility of KNO_3 in $RbNO_3$ IV is about 5 mol %. When annealed, the $RbNO_3$ IV solid solution exsolved from $K_{0.20}Rb_{0.80}NO_3$ and the solubility of $RbNO_3$ in KNO_3 II reduced to 67 mol % (Fig. 3II). The routine Raman measurements over the whole spectrum (Figs 1 and 2) support these solid solubilities, and the Raman studies are consistent with the observations by other techniques [6–8], especially the thermal analysis heating run.

The sample $K_{0.10}Rb_{0.90}NO_3$ manifests interesting properties. Judged by the Raman bands in the ν_1 region, there was a considerable amount of the solid solution with the KNO_3 III structure in the quenched $K_{0.10}Rb_{0.90}NO_3$ (Fig. 3I) but a very small amount of solid solution with the KNO_3 II structure in the annealed

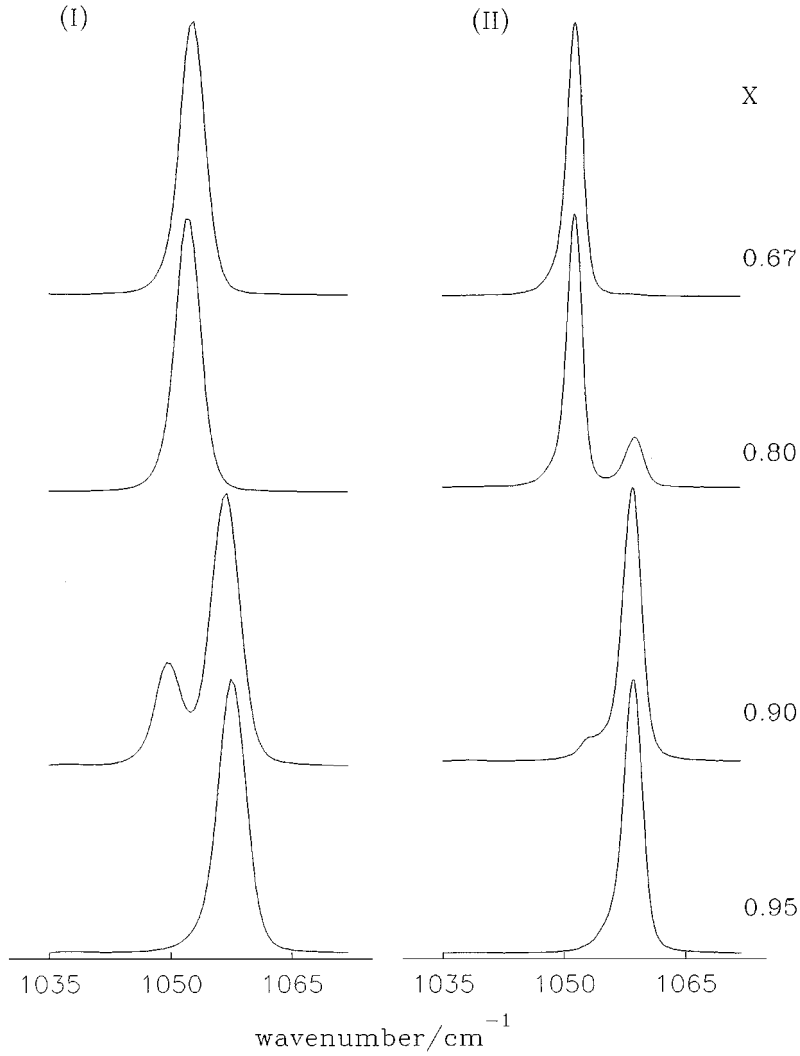

Figure 3 Raman spectra in the ν_1 region of the quenched (I) and annealed (II) $K_{1-x}Rb_xNO_3$ measured at 298 K. x is the mole fraction of Rb^+.

sample (Fig. 3II). The spectrum of the quenched sample was measured first. The spectrum was measured again after annealing. It appears that, after annealing, most of $K_{1-x}Rb_xNO_3$ (KIII) in the quenched $K_{0.10}Rb_{0.90}NO_3$ transformed to $K_{1-x}Rb_xNO_3$ (RbIV) instead of (KII). The remaining small peak due to $K_{1-x}Rb_xNO_3$ (KII) shifted to higher frequency so that it became a shoulder on the band due to $K_{1-x}Rb_xNO_3$ (RbIV). Usually the transition of the KNO_3 III structure to the KNO_3 II structure causes ν_1 to shift to lower frequency [10].

The Raman spectra from 40 to 1800 cm^{-1} by routine measurement showed more clearly the mixed transition of $K_{1-x}Rb_xNO_3$ (KIII) to (RbIV) in $K_{0.10}Rb_{0.90}NO_3$. The distinct Raman features in the ν_1 and ν_4 regions due to the KNO_3 III structure in the quenched sample (Fig. 1b) seemed to disappear completely and there appeared to be only the Raman bands of the $RbNO_3$ IV structure in the annealed sample (Fig. 2c). The annealed $K_{0.05}Rb_{0.95}NO_3$ and $K_{0.10}Rb_{0.90}NO_3$ had such similar Raman spectra by routine measurement (Fig. 2c and d) that at first we assumed that all the KNO_3 III solid solution had transformed to the $RbNO_3$ IV solid solution and the solubility of KNO_3 II in $RbNO_3$ IV was 10 mol %. However, the detailed Raman studies indicated that the latter was a mixture while the former was a single solid solution (Fig. 3II).

The mixed transition of $K_{1-x}Rb_xNO_3$ (KIII) to (RbIV) suggests that the solid solutions with the $RbNO_3$ structure at the high temperature behaved as KNO_3 I. This is possible because $RbNO_3$ II has the same structure as KNO_3 I [2]. When quenched they transformed to the intermediate KNO_3 III structure and when annealed, to the $RbNO_3$ IV structure. Since the overwhelming component in the solid solutions with the KNO_3 III structure in the quenched $K_{0.20}Rb_{0.80}NO_3$ and $K_{0.10}Rb_{0.90}NO_3$ was $RbNO_3$, the crystal of rubidium nitrate might well be regarded as the host in these solid solutions. The changes brought about by quenching or annealing might well be the structural phase transitions involving the $RbNO_3$ structure. This may account for mergence of the Raman features of the KNO_3 III structure into those of the $RbNO_3$ IV in the external and ν_3 regions, as was observed in the spectra of the quenched $K_{0.10}Rb_{0.90}NO_3$ and annealed $K_{0.20}Rb_{0.80}NO_3$ (Figs 1b and 2b). Later we found that the annealed $K_{0.20}Rb_{0.80}NO_3$ was a metastable intermediate phase consisting of a mixture of $K_{1-x}Rb_xNO_3$ (KIII) and (RbIV). It appeared that $K_{1-x}Rb_xNO_3$ (RbIV) exsolved from the quenched $K_{0.20}Rb_{0.80}NO_3$ (KIII) during the 24-h annealing. The remained solid solution retained the KNO_3 III structure. After much longer annealing (a week), the remained solid solution

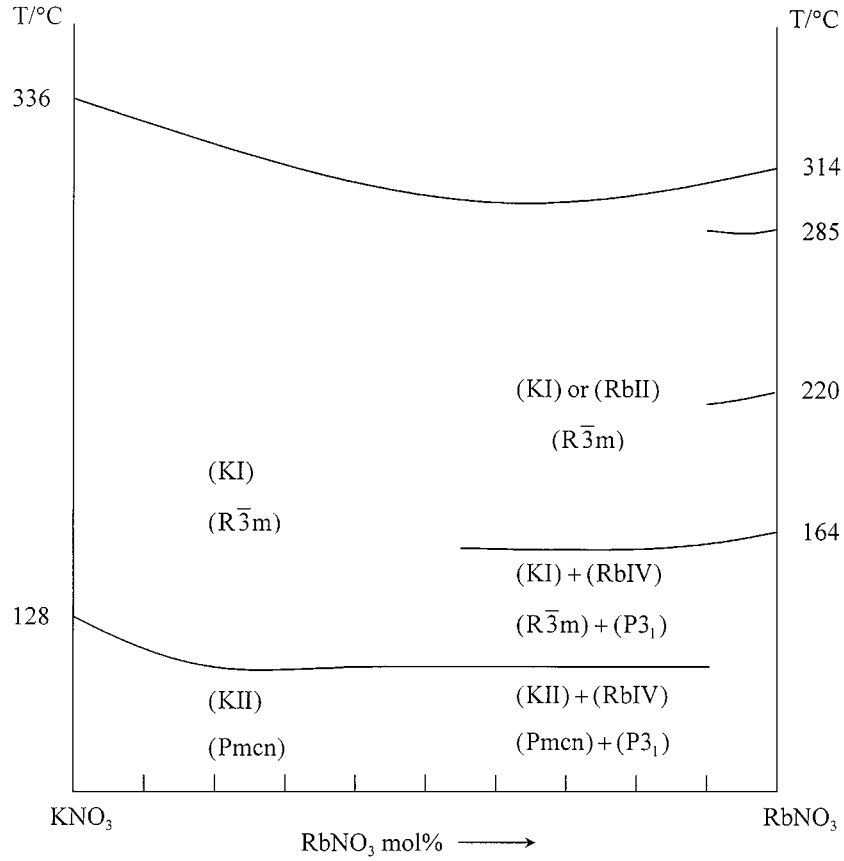

Figure 4 The phase diagram of KNO_3-$RbNO_3$ by DTA heating runings [6]. Raman studies suggest that $RbNO_3$ IV transforms to $RbNO_3$ II in the region of 60 to 90 mol % $RbNO_3$. (KI), (KII), (RbII), and (RbIV) indicate the solid solutions with the KNO_3 I, KNO_3 II, $RbNO_3$ II, and $RbNO_3$ IV structures, respectively.

transformed to the KNO_3 II structure. Fig. 3II is the Raman spectra of one-week annealed samples. It was found that in the ν_1 region the relative intensity due to the KNO_3 structure became much stronger (Figs 2c and 3II) and the doublet feature of KNO_3 II appeared in the ν_3 region.

Raman studies offer a possible explanation for the disappearance of the two transitions of $RbNO_3$ at high temperature in the composition range between 60 and 90 mol % $RbNO_3$ (Fig. 4). The metastable R3m phase with $RbNO_3$ as the host was detected by the Raman technique for quenched $K_{1-x}Rb_xNO_3$ ($x = 0.80$ and 0.90). On annealing, the R3m phase transformed to the $RbNO_3$ IV structure. It would be expected that the reverse process should take place when the mixtures were heated and $K_{1-x}Rb_xNO_3$ (RbIV) transformed to (RbII) which had the same structure as KNO_3 I. Electrical conductivity study also indicated that $K_{1-x}Rb_xNO_3$ (RbII) transformed directly to (RbIV) on cooling when the potassium content was more than 6 mol % [7]. Primary studies of the temperature dependence of $K_{0.20}Rb_{0.80}NO_3$ in our laboratory found that the mixture became one phase (the presumed R$\bar{3}$m) above 420 K. Thus, the missing transitions of rubidium nitrate were phase IV to III and phase II to I (Fig. 4). $RbNO_3$ II and KNO_3 I have the same R$\bar{3}$m structure, and they form continuous solid solutions below the solidus.

The direct transition between the $P3_1$ and R$\bar{3}$m phases and the presence of the metastable KNO_3 III structure in the $RbNO_3$ solid solutions indicated a greater tendency for rubidium nitrate to have the structure of potassium nitrate. This tendency at least partly explains the strikingly different solubilities. It is energetically unfavourable for mixtures of different structures to form solid solutions because the guest member is forced to have the structure of the host member. Usually only limited solubilities are observed for non-isostructural systems. Obviously, it is much easier to force $RbNO_3$ to have the KNO_3 structures than vice versa, resulting in the unusual solid solubilities.

The lattice seemed to be more expanded by Rb^+ in the metastable KNO_3 III structure than in the KNO_3 II structure, because the nitrate ions appeared more sensitive to substitution of rubidium ions. The ν_1 mode of the nitrate ion shifted about 3 cm^{-1} to lower frequency in $K_{1-x}Rb_xNO_3$ (KIII) while it was practically unchanged in $K_{1-x}Rb_xNO_3$ (KII). The 85 cm^{-1} band of KNO_3 II and the 125 cm^{-1} band of KNO_3 III involve the same rotatory modes of the nitrate group [10]. When x increased from 0.05 to 0.67, the frequency of the rotatory modes decreased by 7 cm^{-1} for $K_{1-x}Rb_xNO_3$ (KIII) and by 4 cm^{-1} for $K_{1-x}Rb_xNO_3$ (KII).

The more sensitive response of the KNO_3 III structure to substitution of larger rubidium ions is consistent with the crystallographic studies of the structures and structural phase transitions of potassium nitrate. It was found [8] that both the molar volume and the distance between successive K planes were smaller in KNO_3 III than in KNO_3 II. The more compact KNO_3 III would expand even more when larger rubidium ions

replace smaller potassium ions. The more expanded KNO_3 III would cause larger frequency shifts in the Raman spectrum. Furthermore, the arrangement of the nitrate ions and the cations makes KNO_3 III more sensitive than KNO_3 II to substitution of larger cations. In the KNO_3 III crystal, the potassium ion and nitrate ion alternatively line along the same *c* axis. In the KNO_3 II crystal they are located on different *c* axes, each of which carries only one kind of ion.

The greater expansion in the lattice of KNO_3 III due to larger rubidium ions may partly account for the reported deterioration of ferroelectricity in $K_{1-x}Rb_xNO_3$ (KIII) with increasing contents of $RbNO_3$ [8]. The ferroelectric hysteresis loop and the spontaneous polarization disappeared almost completely when the mole fraction of Rb^+ reached to 0.56. The changes were not considered to be due to the appearance of another crystallographic structure. In this work the Raman spectra of the solid solutions containing $RbNO_3$ up to 80 mol % had practically the same pattern as KNO_3 III even in the most characteristic ν_3 region [10, 11]. It has been reported [11] that the substitution of 30 mol % K^+ by Rb^+ only brought about a very slight broadening of the TO-LO features and about 2 cm^{-1} shift to lower frequencies for both features, which was in good agreement with our observations. Since Raman studies indicated little crystallographic change in the solid solutions, the deterioration in ferroelectricity must be due to some change in the R3m lattice because of the larger rubidium ions.

The disappearance of ferroelectricity may be due to the presence of sufficient number of rubidium ions to overturn the ordering of ferroelectric micro domains in KNO_3 III, to give a structure that resembles KNO_3 I. Both Raman and infrared studies [10, 12] have indicated that it was not appropriate to describe the vibrational spectrum of KNO_3 I on the basis of the average R3m structure determined crystallographically. The R3m structure appears to be the most possible one for the paraelectric KNO_3 I. The TO-LO splitting has been reported [13] in the ν_3 region of the Raman spectrum of KNO_3 I and infrared studies [14] suggested that the local environment of the nitrate ion was practically identical in phases I and III of potassium nitrate. The frequency shift was found to be extremely small and the ν_3 region was essentially unchanged between phases I and III in the IR spectra. It was suggested that the transition of phase I to III involved ordering of dipoles already existing in phase I. This was supported by the study of X-ray diffuse scattering [15] of potassium nitrate above the ferroelectric Curie point.

The thermal transition of KNO_3 III to I was accompanied by large expansion along the *c* axis [16]. Assuming that the expansion of the *c* axis in the solid solutions due to larger rubidium ions had the same effect as the thermal expansion, an addition of 60 mol % $RbNO_3$ would have the same result as a temperature increase of 100 K. It is reasonable to assume that at high concentrations of $RbNO_3$ the ordering of the R3m microstructures in $K_{1-x}Rb_xNO_3$ (KIII) was disrupted, causing the paraelectric properties similar to KNO_3 I.

Recently, theoretical and experimental studies [14, 16, 17] have been directed toward methods to stabilize ferroelectric ordering in KNO_3. The work has focused on thin films of KNO_3 because of their potential applications in random access memory devices. Several mechanisms have been suggested to improve the stability of KNO_3 films in phase III, based on changes in physical properties [17] such as hydrostatic pressure and film thickness. The present work might shed light from the view point of structure. The nitrates of sodium, potassium and rubidium all have the same $R\bar{3}m$ structure at high temperature but only KNO_3 gives rise to a ferroelectric structure on cooling. The size of the cation must be one of the important factors and insertion of small amounts of rubidium ion may lead to stabilized ferroelectric KNO_3 III films.

5. Conclusions

Raman spectroscopic studies of the KNO_3-$RbNO_3$ system revealed the following structural features of the nitrates and their solid solutions:

1. The solubility of $RbNO_3$ was 67 mol % in KNO_3 II and 80 mol % in KNO_3 III. The solubility of KNO_3 in $RbNO_3$ IV was ca. 5 mol %.
2. The transition from R3m to $P3_1$ was observed for samples containing 90 and 80 mol % $RbNO_3$. The tendency of $RbNO_3$ to have the structure of KNO_3 appears to explain why the larger Rb^+ has much greater solubility in KNO_3 than smaller K^+ in $RbNO_3$.
3. $K_{1-x}Rb_xNO_3$ (KIII) was expanded more than $K_{1-x}Rb_xNO_3$ (KII) by larger Rb^+. The greater and uneven expansion in $K_{1-x}Rb_xNO_3$ (KIII) could partly account for the reported deterioration of ferroelectricity as larger rubidium ions were introduced in the crystal.

References

1. J. K. NIMMO and B. W. LUCAS, *J. Phys. C: Solid State Phys.* **6** (1973) 201.
2. M. AHTEE and A. W. HEWAT, *Phys. Stat. Sol.* **a58** (1980) 525.
3. A. C. McLAREN, *Rev. Pur. Appl. Chem.* **12** (1962) 54.
4. A. N. KIRQUINTSEV and N. YA. YACOBI, *Russ. J. Inorg. Chem.* **16** (1971) 1681.
5. B. D. STEPIN, Z. A. STANIKOVA, A. N. KNYAZEVA, G. A. LOVETSKAYA and V. K. TRUNOV, *Russ. J. Inorg. Chem.* **23** (1978) 126.
6. P. I. PROTSENKO, L. S. GRIN'KO, L. N. VENEROVSKAYA and V. A. LYUTSEDARSKII, *J. Appl. Chem. USSR* **46** (1973) 2568.
7. P. P. SALHOTRA, E. C. SUBBARAO and P. VENKATESWARLU, *J. Phys. Soc. Jpn.* **27** (1969) 621.
8. U. KAWABE, T. YANAGI and S. SAWADA, *ibid.* **20** (1965) 2059.
9. N. A. PUSCHIN and M. RADOICIC, *Z. Anorg. Alig. Chem.* **233** (1937) 41.
10. M. H. BROOKER, *J. Phys. Chem. Solids* **39** (1978) 657.
11. J. P. DEVLIN and R. FRECH, *J. Chem. Phys.* **63** (1975) 1663.
12. F. BREHAT and B. WYNCKE, *J. Phys.* **C21** (1988) 689.
13. J. P. DEVLIN and D. W. JAMES, *J. Chem. Phys.* **53** (1970) 4394.
14. M. J. HARRIS, *Solid State Commun.* **84** (1992) 557.
15. Y. SHINNAKA, *J. Phys. Soc. Jpn.* **17** (1962) 820.
16. H. M. LU and J. R. HARDY, *Phys. Rev.* **B44** (1991) 7215.
17. J. F. SCOTT *et al.*, *ibid.* **B35** (1987) 4044.

Received 17 June 1998
and accepted 26 January 1999